Colloids and Surfaces B: Biointerfaces 95 (2012) 214–221

Contents lists available at SciVerse ScienceDirect

Colloids and Surfaces B: Biointerfaces

journal homepage: www.elsevier.com/locate/colsurfb

Interfacial and foaming interactions between casein glycomacropeptide (CMP) and propylene glycol alginate

María J. Martinez[a], Víctor M. Pizones Ruiz-Henestrosa[a], Cecilio Carrera Sánchez[b], Juan M. Rodríguez Patino[b], Ana M.R. Pilosof[a,*]

[a] Departamento de Industrias, Facultad de Ciencias Exactas y Naturales, Universidad de Buenos Aires, Avenida Intendente Güiraldes s/n, Ciudad Universitaria (1428), Buenos Aires, Argentina

[b] Departamento de Ingeniería Química, Facultad de Química, Universidad de Sevilla, C/Prof. García González, 1, (41012) Sevilla, Spain

ARTICLE INFO

Article history:
Received 20 January 2012
Received in revised form 28 February 2012
Accepted 29 February 2012
Available online 7 March 2012

Keywords:
Casein glycomacropeptide
Propylene glycol alginates
Interface
Foam

ABSTRACT

Proteins and polysaccharides are widely used in food formulation. While most of the proteins are surface active, only few polysaccharides can adsorb at the air–water interface; this is the case of propylene glycol alginates (PGA). It is known that casein glycomacropeptide (CMP), a bioactive polypeptide derived from κ-casein by the action of chymosin, presents a great foaming capacity but provides unstable foams. So, the objective of this work was to analyze the impact of mixing CMP and a commercial variety of PGA, Kelcoloid O (KO), on the interfacial and foaming properties at pH 7.0. It was determined the surface pressure isotherm, the dynamics of adsorption and the foaming properties for CMP, KO and the mixed system CMP–KO.

CMP dominated the surface pressure of CMP–KO mixed system. The presence of KO synergistically improved the viscoelastic properties of surface film. The foaming capacity of CMP was altered by KO. KO foam presented a higher stability than CMP foam and it controlled the stability against drainage and the initial collapse in the mixed foam.

1. Introduction

Several processed foods are multiphase systems which contain two or more immiscible phases (aqueous, oil, or gas) in the form of foams and emulsions. Foams are heterogeneous systems consisting of a gas phase dispersed into an aqueous phase, for example, air in water. The interest in understanding the physical and chemical mechanisms responsible for the foam formation and stability has increased in recent years since most consumers appreciate the soft and creamy mouth sensations triggered by foam structures. The formation and stability of foams is generally achieved through a protective interfacial layer of surface-active substances around the air bubbles.

Casein glycomacropeptide (CMP) is a heterogeneous fraction of peptides formed by the action of rennet on κ-casein and next to β-lactoglobulin and α-lactalbumin is the most abundant protein/peptide (20% and 25% of the proteins) in whey products manufactured from cheese whey [1,2]. The formulation of foams containing CMP is of great interest because of possible health-promoting benefits [1–3]. Additionally, CMP lacks Phe in its amino acid composition, so it is suitable for nutrition for people suffering from phenylketonuria [1].

It is known that CMP has great foaming capacity which may be accounted for by the high surface activity of CMP as compared to other whey proteins, like β-lactoglobulin [4,5]. However foams are unstable [6,7]. There exist non-glycosylated (aCMP) and glycosylated (gCMP) forms of CMP with values of pI close to 4.1 and 3.15, respectively [8].

CMP fractions (both aCMP and gCMP) were studied by Kreuβ, et al. [8,9] for their foaming and emulsifying properties, respectively. They found that aCMP showed better interfacial properties than gCMP and that the pH influenced some of these properties especially near to pI.

Therefore, to use CMP in foamed products a good strategy must be developed to improve foam stability. Polysaccharides are generally used to this end because they impart viscosity to the foam, thus retarding its destabilization. Nevertheless, some specific polysaccharides exhibit surface activity that allows the formation of stable foams. Propylene glycol alginates (PGA) are an example of polysaccharides used in food foams, such as beer. PGA is a derivative of the reaction between propylene oxide and alginic acid to produce a partial ester with 50–85% of the carboxyl groups esterified. The

* Corresponding author. Tel.: +54 11 45763377; fax: +54 11 45763366.
E-mail addresses: mjm@di.fcen.uba.ar (M.J. Martinez), vicpizrui@di.fcen.uba.ar (V.M. Pizones Ruiz-Henestrosa), cecilio@us.es (C. Carrera Sánchez), jmrodri@us.es (J.M. Rodríguez Patino), apilosof@di.fcen.uba.ar (A.M.R. Pilosof).

0927-7765/$ – see front matter © 2012 Elsevier B.V. All rights reserved.
doi:10.1016/j.colsurfb.2012.02.045

interfacial and foaming properties of these polysaccharides were previously studied [10]. The stability of the foams formed by PGA depends on the combined effect of molecular weight and degree of esterification, on the viscosity and also viscoelasticity of the adsorbed film.

The aim of this work was to study the effect of propylene glycol alginate addition on CMP foams and interfaces.

When a protein adsorbs at a fluid interface in the presence of a surface-active polysaccharide, like PGA, in conditions of bulk thermodynamic incompatibility (i.e. pH above protein pI) three phenomena can occur [11]:

(1) The polysaccharide adsorbs at the interface and increases the surface pressure in competition with the protein (competitive adsorption). It has been reported the competitive adsorption between proteins and low-molecular-weight surface active agents such as monoglycerides [12,13], lecithins [14], surfactants [15,16] and surface active polysaccharides like propylene glycol alginates [17].
(2) The complexation of the polysaccharide with the adsorbed protein at the interface [18], which can occur by slight electrostatic or hydrophobic interactions.
(3) The existence of a limited thermodynamic compatibility between protein and polysaccharide which provokes an increment of the adsorbed macromolecules concentration [17,19–22].

2. Materials and methods

2.1. Single and mixed solutions

BioPURE GMP casein glycomacropeptide was provided by DAVISCO Foods International, Inc. (Le Sueur, Minnesota). Its composition was: protein (dry basis) 79.0% being CMP 86.3% of total proteins, fat 0.6%, ash 6.3% and moisture 6.4%. Kelcoloid O (KO) is a commercial variety of propylene glycol alginate and it was provided by ISP Alginates (San Diego, CA, United States). The degree of esterification of KO, given by the supplier, is high (78–85%).

CMP and KO solutions were prepared freshly by dissolving the proper amount of powders in Trizma $(CH_2OH)_3CNH_2/(CH_2OH)_3CNH_3Cl$ (Sigma, >99.5%) buffer at pH 7.0, and Milli-Q ultrapure water at room temperature and stirring for 30 min. Ionic strength in all the experiments was 0.05 M. The CMP:KO mixed systems were prepared by mixing the appropriate volume of each protein solution up to achieve a required concentration. Finally the solutions were kept 24 h at 4 °C before measurements.

The materials in contact with the protein solutions were properly cleaned in order to avoid any contamination by any surface-active substance. The absence of surface-active contaminants in the aqueous buffered solutions was checked by surface tension measurements before sample preparation. No aqueous solutions with a surface tension other than that accepted in the literature (72–73 mN/m at 20 °C) were used.

2.2. Surface pressure isotherm

Surface tension measurements were used to determine the adsorption of KO and the adsorption of CMP in the presence of KO at the air–water interface at equilibrium. The surface pressure isotherm of CMP was determined previously [4]. These measurements were registered with a Sigma 701 digital tensiometer (KSV Instruments Ltd., Finland), based on the Wilhelmy plate method, with a roughened platinum plate, as described elsewhere [23].

KO solutions in an increased range of bulk concentrations from 1×10^{-4} to 1 wt% were used to obtain the KO adsorption isotherm at pH 7.0. CMP solutions of increasing concentrations from 5×10^{-7} to 5 wt% in the presence of a KO bulk concentration constant at 0.5 wt% were used to determine the adsorption isotherm of the mixed systems. Prior to the measurements, the solutions were allowed to age during 24 h at 4 °C to achieve the biopolymer adsorption.

The temperature was maintained constant at 20 °C within ±0.5 °C by a circulating Heto thermostat. A device connected to the tensiometer recorded the reduction in surface tension, γ, continuously. Equilibrium was assumed when the pressure did not change by more than 0.1 mN/m in 30 min. Surface activity was expressed by the surface pressure (Eq. (1)): $\pi_{eq} = \gamma_0 - \gamma_{eq}$, where, γ_0 and γ_{eq} are the aqueous subphase surface tension and the surface tension at equilibrium of the protein or polysaccharide solutions, respectively. Some experiments were replicated three or four times. It was found that π_{eq} could be reproduced to ±0.5 mN/m.

2.3. Interfacial dynamic properties

The existence of interactions between CMP and KO at the air–water interface was determined by monitoring the dynamics of surface pressure (π) of single components and the mixed systems. Time-dependent surface pressure and surface viscoelastic parameters of adsorbed KO and mixed systems CMP:KO films at the air–water interface were obtained with an automatic drop tensiometer (TRACKER, IT Concept, Longessaine, France) as described elsewhere [24,25].

The aqueous solutions of KO or CMP:KO were placed in a 15 μL glass Hamilton syringe equipped with a stainless steel needle and then in a rectangular glass cuvette (5 mL) covered by a compartment, which was maintained at constant temperature (20 ± 0.2 °C) by circulating water from a thermostat, and was allowed to stand for 30 min to reach constant temperature and humidity in the compartment. Then a drop of KO or CMP:KO mixed solutions (5–8 μL) was delivered and allowed to stand at the needle tip for about 180 min to achieve biopolymer adsorption at the air–water interface. The image of the drop was continuously taken from a CCD camera and digitized. The surface tension (γ) was calculated through analyzing the profile of the drop [24]. The surface pressure is $\pi = \gamma_0 - \gamma$, where γ is the surface tension of protein solutions.

The surface viscoelastic parameters (surface dilatational modulus, E, and its elastic, E_d, and viscous, E_v, components) were measured with the same drop tensiometer [25] as a function of time, t, at 10% deformation amplitude ($\Delta A/A$) and 100 mHz of angular frequency (ω). The method involved a periodic automated-controlled, sinusoidal interfacial compression and expansion performed by decreasing and increasing the drop volume, at the desired amplitude. The sinusoidal oscillation for surface dilatational measurements were made with five oscillation cycles followed by a time of 50 cycles without any oscillation up to the time required to complete adsorption. The average standard accuracy of the surface pressure is roughly 0.1 mN/m. However, the reproducibility of the results (for two measurements) was better than 0.5%. The surface dilatational modulus derived from the change in interfacial tension (dilatational stress), σ (Eq. (2)): $\sigma = \sigma_0 \sin(\omega t + \delta)$, resulting from a small change in surface area (dilatational strain), A (Eq. (3)): $A = A_0 \sin(\omega t)$, and may be described by Eq. (4): $E = d\sigma/(dA/A) = -d\pi/d \ln A$ [26], where σ_0 and A_0 are the stress and strain amplitudes, respectively, and δ is the phase angle between stress and strain.

The dilatational modulus is a complex quantity and it is composed of real and imaginary parts (Eq. (5)): $E = E_d + iE_v$. The real part of the dilatational modulus or storage component is the dilatational elasticity, $E_d = |E| \cos \delta$. The imaginary part of the dilatational modulus or loss component is the surface dilatational viscosity,

$E_v = |E| \sin \delta$. The ratio (σ_0/A_0) is the absolute modulus (E), a measure of the total unit material dilatational resistance to deformation (elastic + viscous). For a perfect elastic material the stress and strain are in phase ($\delta = 0$) and the imaginary term is zero. In the case of a perfectly viscous material, $\delta = 90^\circ$ and the real part is zero.

2.4. Foaming properties

The determination of foaming properties (foam formation and foam stability) was performed using a commercial instrument (Foamscan™, Teclis, Logessaigne, France). This instrument allows us to characterize the foam formation, the foam volume stability and the drainage of liquid from the foam by conductimetric and optical measurements as it was described in a previous work [27]. The foam is generated by blowing gas (nitrogen) at a flow of 45 mL/min through a porous glass filter (pore diameter 0.2 μm) at the bottom of a glass tube where 25 mL of the foaming aqueous solution is placed. In all experiments, the foam was allowed to reach a volume of 120 mL. The bubbling was then stopped and the evolution of the foam was analyzed. Foaming properties were measured at 20 ± 1 °C. The generated foam rises along a thermostated square prism glass column, where its volume is followed by image analysis using a CCD camera. The amount of liquid incorporated in the foam, the foam homogeneity, and the liquid drainage from the foam are followed by measuring the conductivity in the cuvette containing the liquid sample and at different heights in the glass column by mean of electrodes.

Two parameters were determined as a measure of foaming capacity. The overall foaming capacity (OFC) was determined from the slope of the foam volume curve up to the end of the bubbling. The foaming capacity (FC), which is a measure of gas retention in the foam, was determined by Eq. (6): $FC = (V_{foam(f)})/(V_{gas(f)})$, where $V_{foam(f)}$ is the final foam volume, $V_{gas(f)}$ is the final gas volume injected, respectively.

The static foam stability was determined from the volume of liquid drained from the foam over time [28]. The half-life time ($t_{1/2}$), referring to the time needed to drain half of the volume of the liquid in the foam, was used as a measure of foam stability.

The foam stability was also determined by following the development of the bubble size in the foam. The foamscan apparatus is equipped with a second CCD camera set having a macro objective to capture the variation of the air bubble size of the foam every 5 s at a foam height of about 10 cm (half of the foam height).

All the experiments were performed in duplicate. The reported values are the average and standard deviation of them.

3. Results and discussion

3.1. Surface pressure isotherm of KO

Fig. 1 shows the effect of KO concentration (C_{KO}) on the equilibrium surface pressure at pH 7.0. As for proteins [4,29,30] and other polysaccharides [31] true equilibrium adsorption does not seem to be possible with this polysaccharide, therefore it was assumed the pseudo equilibrium value for the surface pressure measured after 24 h.

The behavior observed for KO solutions at pH 7.0 was sigmoidal which is typical for biopolymers and surfactants [20,31–33]. The surface pressure increased with KO concentration, showing surface activity from bulk concentration of 1×10^{-4} wt%.

The surface pressure increased slightly from 1×10^{-4} to 1×10^{-2} wt% and then the slope increased strongly. An inflexion point is observed at 1×10^{-1} wt% (C_{crit}). As it was explained in a previous work [4] this inflexion point in the π–C isotherms is related with a change in the conformation of the adsorbed macromolecule

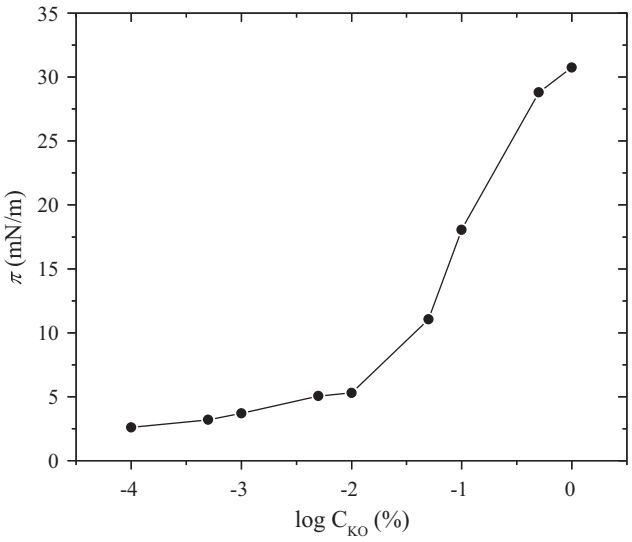

Fig. 1. Surface pressure isotherm for KO. Temperature 20 °C, pH 7.0 and $I = 0.05$ M.

[31,34]. So, at surface pressure below 11 mN/m (π_{crit}) KO would adopt and expanded structure and above this surface pressure a more condensed conformation would be attained.

Pérez et al. [31] studied different types of hydroxypropyl-methyl-celluloses (HPMC) and they found similar values of surface pressure as KO for the higher concentrations, however HPMC showed lower transition concentrations compared with KO. The differences in C_{crit} and π_{crit} are related to molecular features and with the molecular mass (PGA < HPMC).

The monolayer saturation was not reached even at 1 wt% bulk concentration, as indicated by the absence of a plateau [20,32].

3.2. Surface pressure isotherm of CMP in the presence of KO

CMP:KO interactions at the air–water interface were analyzed in mixed systems as a function of CMP concentration (from 5×10^{-6} to 4 wt%) and at constant KO concentration (of 0.5 wt%). Fig. 2 shows the surface pressure isotherm for CMP in the presence of KO. In this

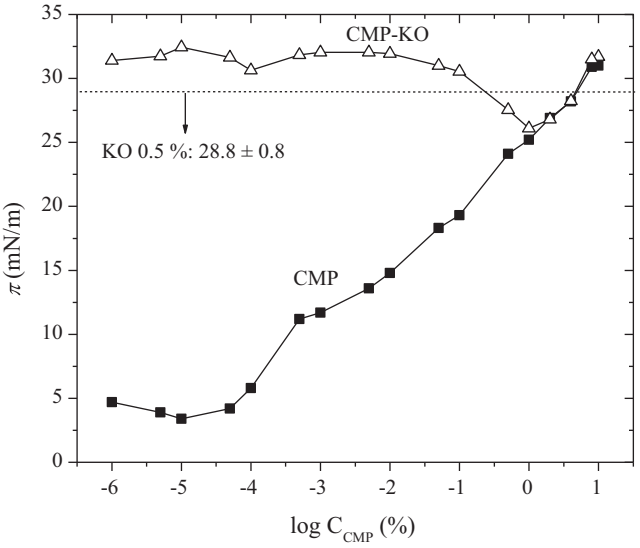

Fig. 2. Surface pressure isotherm for (■) CMP alone and (△) CMP in the presence of KO (0.5 wt%). The dotted line corresponds to the equilibrium surface pressure value of KO at 0.5%. Temperature 20 °C, pH 7.0 and $I = 0.05$ M.

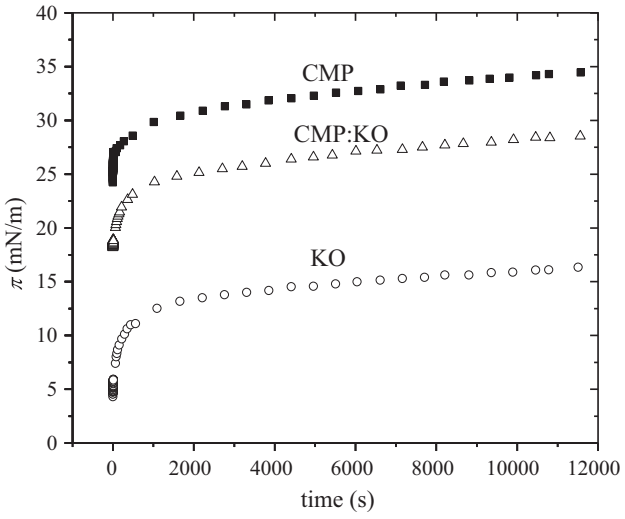

Fig. 3. The transient surface pressure (π) for (■) CMP 4 wt%, (○) KO 0.5 wt% and (△) CMP:KO at concentration 4 wt%:0.5 wt% adsorbed at the air–water interface. Temperature 20 °C, pH 7.0 and I = 0.05 M.

figure it was also plotted the surface pressure isotherm of pure CMP [4] for comparison purpose.

It is possible to observe that KO determined the equilibrium surface pressure of the mixed systems at CMP concentrations lower than 0.1 wt%, showing the mixed systems surface pressure values close to the solution of KO at 0.5 wt% (dot line in Fig. 2), which is the concentration used in the mixtures. At CMP concentrations above 1 wt%, the surface activity was clearly dominated by CMP. The influence of CMP on the surface pressure of the mixture is evident in Fig. 2 from a ratio CMP:KO higher than 2:1.

3.3. Adsorption dynamics

For the dynamic interfacial measurements as well as for foam formation, CMP and KO concentrations of 4 wt% and 0.5 wt% respectively were used. According to Fig. 2 in these conditions the equilibrium surface pressure of mixture is dominated by CMP.

The dynamics of adsorption of KO and the mixed system with CMP was determined by measurements of surface pressure (π) over time. The evolution of the surface pressure of this mixed system as well as of CMP and KO alone is shown in Fig. 3.

Surface pressure immediately increased after drop formation. This behavior is associated with the adsorption of the protein [35–37] and the polysaccharide [10,17] at the air–water interface. The surface pressure of CMP–KO solution was closer to single CMP (Fig. 3). As KO is less surface active than CMP at these concentrations, the replacement of CMP at the interface by KO resulted in lower surface pressure. Nevertheless a competitive behavior exists between both macromolecules during adsorption.

The main step of the kinetics of adsorption of macromolecules include [34,38–40]: (i) the diffusion of the macromolecule from the bulk onto the interface, (ii) adsorption (penetration) and interfacial unfolding, and (iii) association (rearrangement) within the interfacial layer, multilayer formation and even interfacial gelation. At low surface concentration, surface pressure is low and molecules adsorb irreversibly by diffusion. Thus, during the first step, at relatively low surface pressures, when diffusion is the rate-determining step (if π value is lower than 10 mN/m), a modified form of the Ward and Tordai equation can be used to correlate the change in surface pressure with time [41] (Eq. (7)): $\pi = 2C_0KT\,(D_{diff}t/3.14)^{1/2}$, where C_0 is the concentration in the aqueous phase, K the Boltzmann constant, T the absolute temperature, D_{diff} the diffusion coefficient, and t the adsorption time. If the diffusion at the interface controls the

Table 1
Rate constant of diffusion (k_{diff}) for KO, CMP and CMP:KO mixture at 20 °C, pH 7.0 and at ionic strength 0.05 M.

	k_{diff} (mN m^{-1} s$^{-0.5}$)[a] (LR)
CMP	>76.72 ± 1.21[b]
KO	0.31 ± 0.04 (0.944)[c]
CMP:KO	>66.23 ± 3.12[b]

LR: Linear regression coefficient.
[a] Mean ± standard deviation.
[b] Calculated from the slope of the first point of a plot of π against time$^{1/2}$.
[c] Calculated by Eq. (7).

adsorption process, a plot of π against time$^{1/2}$ will then be linear [38,42–44] and the slope of this plot will be the diffusion rate (k_{diff}). For KO solution it is possible to use the Eq. (7), which means that the adsorption kinetics of KO to the air–water interface is controlled by the diffusion step, which is in agreement with previous results for this and other polysaccharides [10]. The opposite was observed for CMP (4 wt%) [4] and the mixed system, which showed a diffusion step too fast (π > 10 mN/m) to be detected by this experimental technique. These results suggest that the adsorption kinetics of the protein and the mixed system at these concentrations was not driven by the diffusion step. As it was explained in a previous work on CMP [4] for initial π values higher than 10 mN/m, it was possible to obtain an estimation of the diffusion rate constant (k_{diff}) from the slope of the first point in a plot of π against time$^{1/2}$. The values of k_{diff} are shown in Table 1. CMP and the mixed system showed a very fast and similar diffusion that is characteristic of low-molecular-weight surfactants [32,45]. It is possible to conclude that CMP dominates at the beginning of the adsorption process because the values of k_{diff} for CMP and the mixed system were similar and much higher than the value of k_{diff} for KO.

After the diffusion step, to analyze the rate of adsorption (penetration) and rearrangement of adsorbed biopolymer a semi empirical first-order equation (Eq. (8)) was used [35]: $\ln[(\pi_{180} - \pi_t)/(\pi_{180} - \pi_0)] = -k_i \cdot t$, where π_{180}, π_0, and π_t are the surface pressures at 180 min of adsorption time, at time t = 0, and at any time t, respectively, and k_i is the first-order rate constant. In practice, a plot of Eq. (8) usually yields two or more linear regions. The fit of the experimental data to obtain the rate of adsorption/penetration (k_{ads}) was made at a time interval based on the

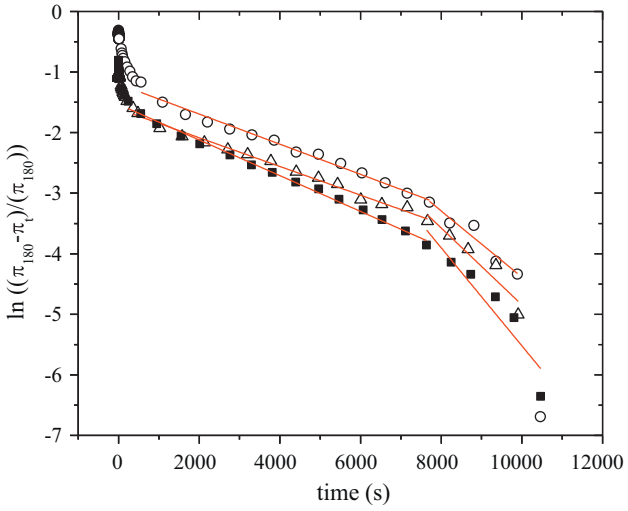

Fig. 4. Time-dependent surface pressure of (■) CMP, (○) KO and (△) the mixed system CMP:KO adsorbed films according to the rate of adsorption, unfolding, and penetration at the air–water interface. Concentration of KO alone and in the mixed system: 0.5 wt%. Concentration of CMP alone and in the mixed system: 4 wt%. Temperature 20 °C, pH 7.0 and I = 0.05 M.

Table 2
Rate constant of adsorption (k_{ads}) and rearrangement (k_r) for CMP, KO and CMP:KO mixture at 20 °C, pH 7.0 and ionic strength 0.05 M.

	$k_{ads} \times 10^4$ (s^{-1})[a] (LR)	$k_r \times 10^4$ (s^{-1})[a] (LR)
CMP	2.56 ± 0.32 (0.996)	7.62 ± 0.47 (0.940)
KO	2.55 ± 0.03 (0.994)	5.65 ± 0.09 (0.984)
CMP:KO	2.50 ± 0.09 (0.996)	5.07 ± 0.63 (0.976)

LR: Linear regression coefficient.
[a] Mean ± standard deviation.

best linear regression coefficient. The initial slope is taken to correspond to a first-order rate constant of adsorption/penetration (k_{ads}), and the second slope corresponds to a first-order rate constant of biopolymer rearrangement (k_r), occurring among a more or less constant number of adsorbed molecules.

Fig. 4 shows the fit of experimental data to Eq. (8) for the three systems studied and Table 2 shows the rate constants for adsorption/penetration and rearrangement obtained from Fig. 4. Regarding the rate of adsorption/penetration it was observed similar values for pure components and the mixed system, while the rearrangement rate was faster for CMP, a phenomenon that can be attributed to the great flexibility of the molecule of CMP [9]. Additionally, the value of k_r for the mixed system was lower than that of CMP indicating that the presence of KO and CMP at the air–water interface lowers the rate of rearrangement.

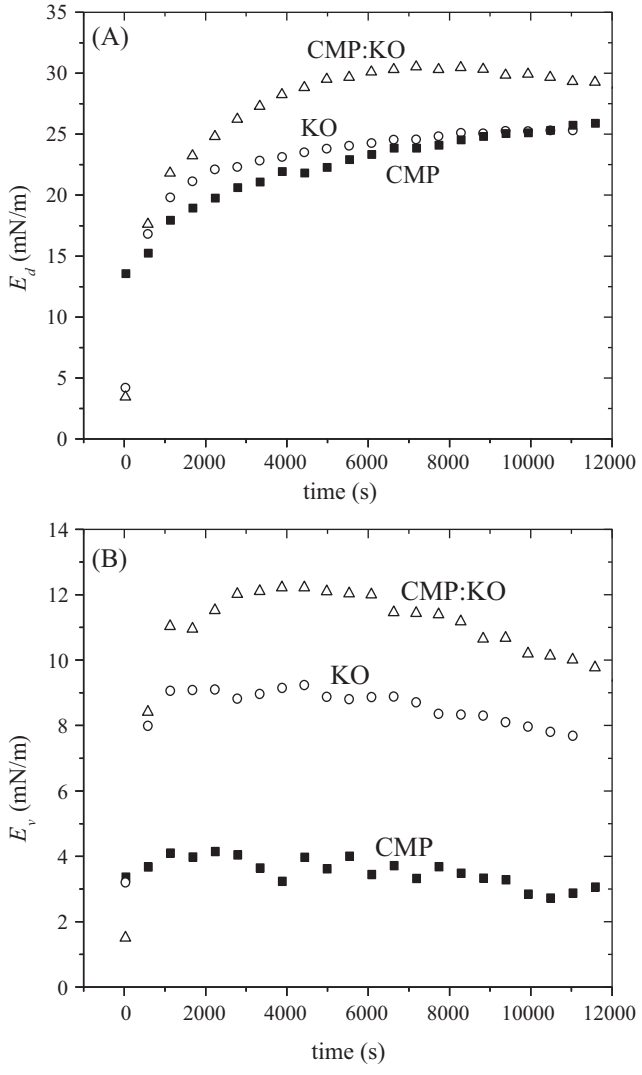

Fig. 5. Time-dependent (A) surface dilatational elasticity, E_d, and (B) surface dilatational viscosity, E_v, for (■) CMP, (○) KO and (△) CMP:KO mixed system adsorbed at the air–water interface. Concentration at the pure solution and mixed system: 4 and 0.5 wt% for CMP and KO, respectively, Frequency 100 mHz. Amplitude of deformation: 10%. Temperature 20 °C, pH 7.0 and I = 0.05 M.

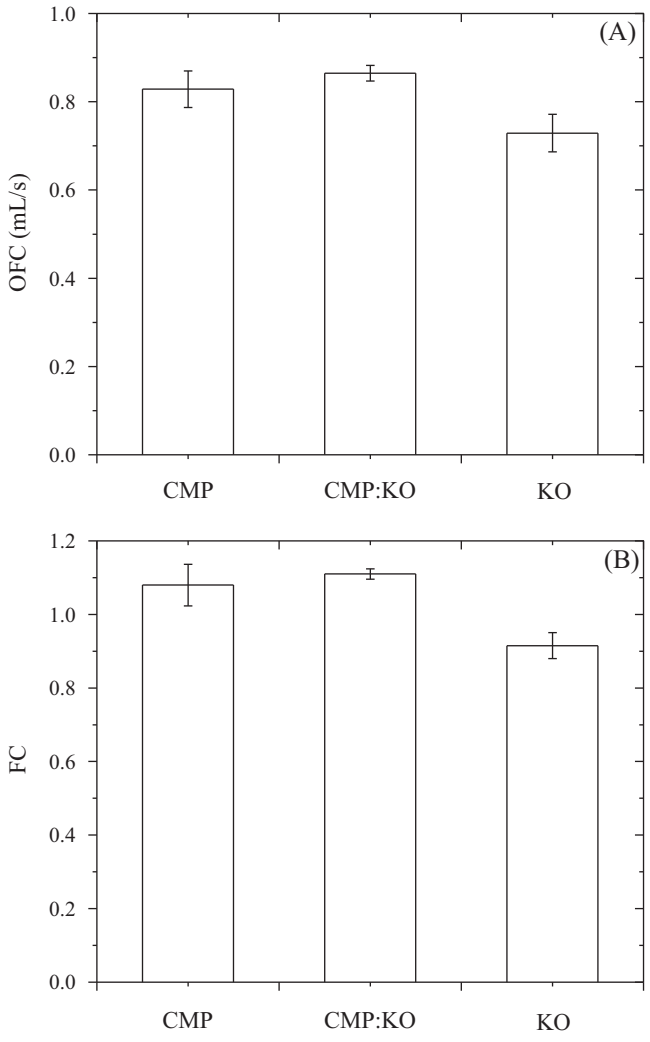

Fig. 6. (A) Overall foam capacity (OFC) and (B) foaming capacity (FC) for foam generated from aqueous solutions of CMP, KO and the mixed system. Concentration at the pure solution and mixed system: 4 and 0.5 wt% for CMP and KO, respectively. Error bar are standard deviations of mean values. Bubbling gas: nitrogen. Gas flow: 45 mL/s. Temperature 20 °C, pH 7.0 and I = 0.05 M.

3.4. Viscoelastic properties of CMP, KO and CMP:KO films

Fig. 5 shows the rheological properties (E_d and E_v) of CMP, KO and CMP:KO surface films. The values of E_d increased with time according to biopolymer adsorption. The pure components presented similar values of E_d (Fig. 5A) while the mixed system CMP:KO showed a higher value. This behavior indicates a synergistic effect between CMP and KO in relation to the elasticity of the film. Similar results were obtained by Baeza et al. [46] in mixed systems of β-lactoglobulin and PGAs and they explained their results in terms of concentration of the protein at the interface due to incompatibility with the polysaccharide, Moreover, it could occur complexation between both macromolecules leading to an increased film thickness with the consequent increase in the elastic modulus. Others authors [47] found results similar to Baeza et al. [46] with an increase in film thickness in BSA/PGA mixed systems

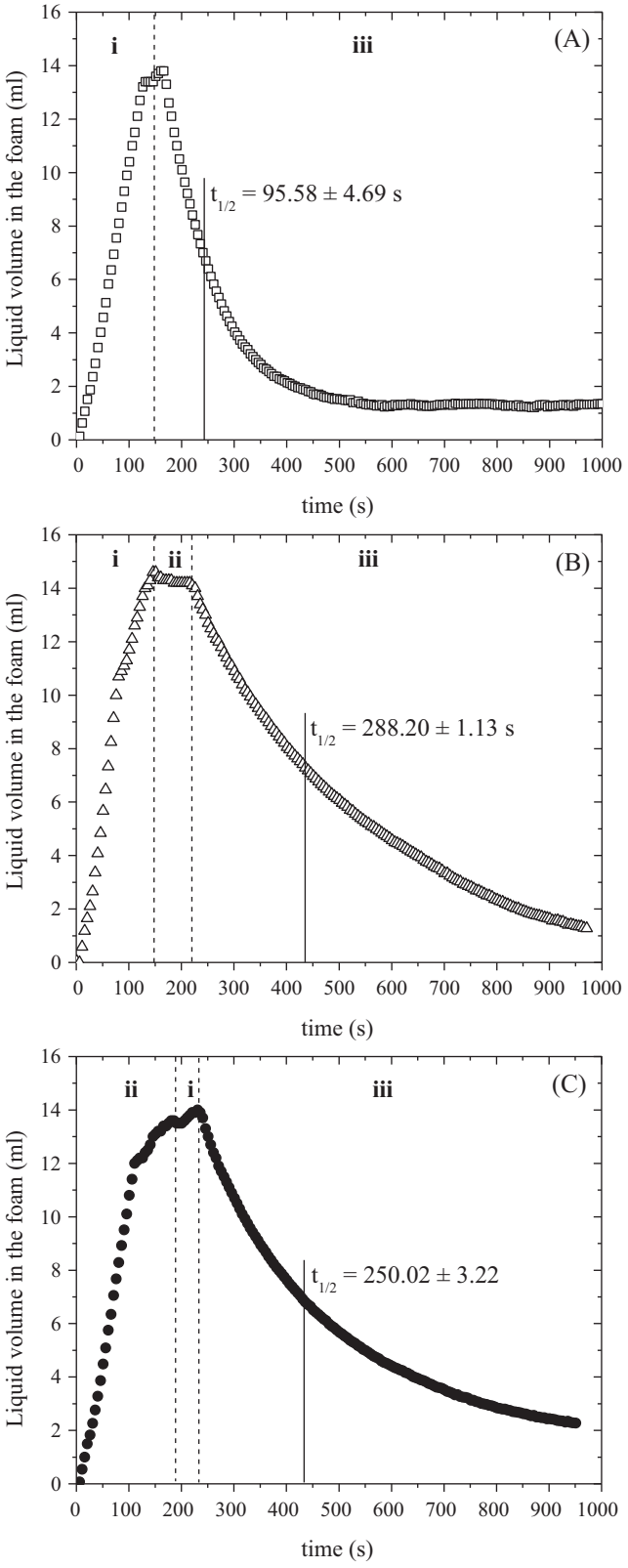

Fig. 7. Liquid volume of the foam as a function of time for foam generated from aqueous solutions of (A) CMP, (B) CMP–KO and (C) KO. Concentration at the pure solution and mixed system: 4 and 0.5 wt% for CMP and KO, respectively. In each plot is indicated the $t_{1/2}$ of drainage of the foam. Bubbling gas: nitrogen. Gas flow: 45 mL/s. Temperature 20 °C, pH 7.0 and I = 0.05 M.

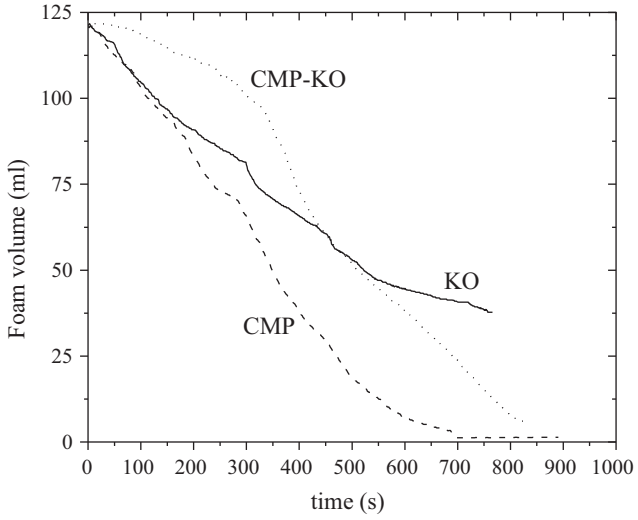

Fig. 8. Foam volume as a function of time for foam generated from aqueous solutions of (- - -) CMP, (···) CMP–KO and (——) KO. Concentration at the pure solution and mixed system: 4 and 0.5 wt% for CMP and KO, respectively. Bubbling gas: nitrogen. Gas flow: 45 mL/s. Temperature 20 °C, pH 7.0 and I = 0.05 M.

which was attributed to polysaccharide association with protein in the adsorbed layer.

The viscous component (Fig. 5B) was also higher for the mixed system compared to pure components although in this case the E_v value of KO was higher than the E_v value of CMP.

As KO is hydrophobic [47] and CMP has hydrophobic regions [8] they could interact strengthening interfacial film. The improvement of the interfacial rheology by complexation between proteins and polysaccharides has been reported [48–52].

3.5. Foaming capacity

Fig. 6 shows the overall foaming capacity which is a measure of the rate of foam formation and the foaming capacity which is a measure of the ability of each solution to retain the gas passing throughout. There is no significant difference between CMP and mixed foam for both parameters; however, OFC and FC values were lower for KO foam. It could be observed that the presence of a low concentration of KO in the CMP solution did not decrease the efficiency of CMP on foaming.

3.6. Foam stability

Fig. 7 shows the change of the liquid volume in the foam that first increases during bubbling and then decreases due to liquid drainage during foam ageing. The variation of the liquid volume in the foam during its generation shows the presence of three stages [53]:

(i) an entrainment stage, when the liquid transfer from the bulk phase to the foam is dominant and the solution is transferred into the foam following a linear law up to the end of the bubbling,
(ii) a steady stage, when entrainment and drainage phenomena are balanced and no liquid is transferred in the foam,
(iii) a drainage stage, when drainage phenomena are dominant so the liquid volume in foam decreased and the bulk phase increased.

In the curve corresponding to CMP foam (Fig. 7A) the steady stage was not present because as soon as the maximum liquid volume is reached the destabilization of the foam starts. However, the

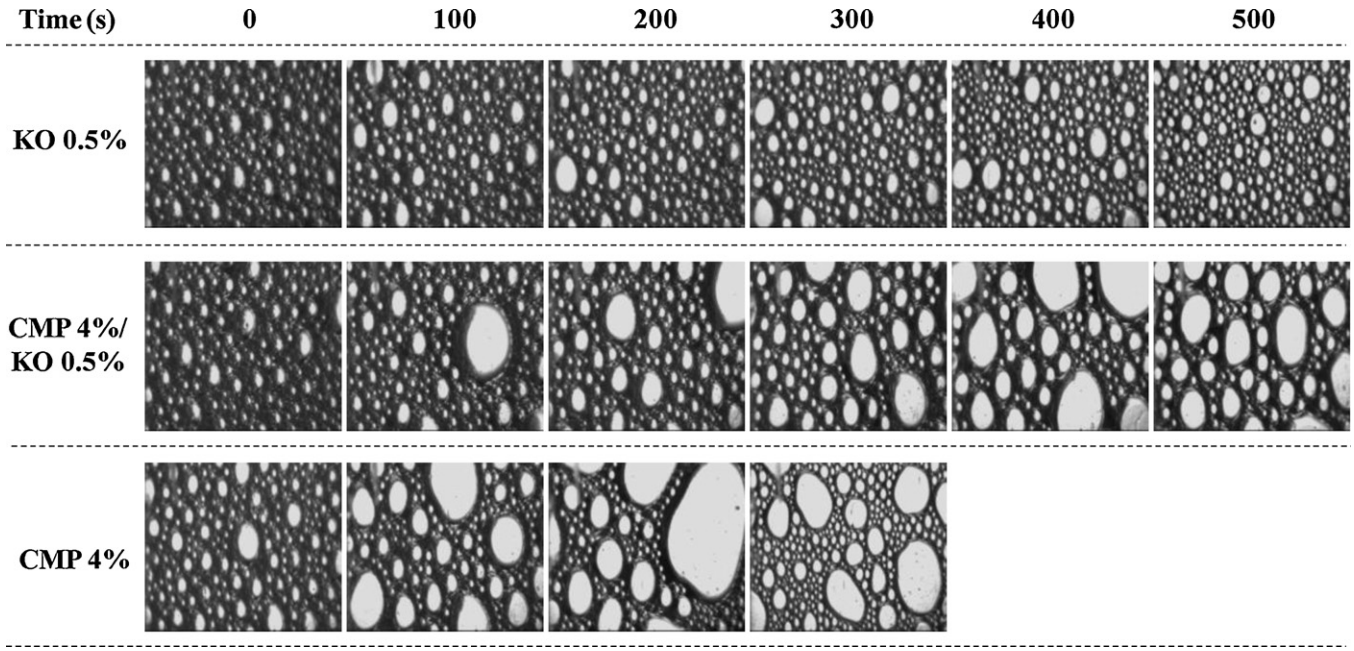

Fig. 9. Light micrographs showing the development with time of air bubbles determined in foams generated from aqueous solutions of CMP, KO and the mixed system CMP–KO. Concentration at the pure solution and mixed system: 4 and 0.5 wt% for CMP and KO, respectively. Temperature 20 °C, pH 7.0 and $I = 0.05$ M.

steady stage was present for CMP–KO and KO foams being more extensive for the mixed foam (steady stage for CMP–KO foam ~72 s, steady stage for KO foam ~46 s) indicating that the mixed system (Fig. 7B) was more stable at the beginning of the drainage, resulting in a more stable foam, which is in agreement with the results of $t_{1/2}$ indicated in each plot. Regarding these values of $t_{1/2}$, KO foam presented much higher stability than CMP foam and the more relevant result was observed for the mixed system which showed the highest stability against drainage. This result suggests that KO controls the drainage stability of the foam. Moreover a synergic effect in the mixed system CMP–KO is apparent. Additionally, it is possible to relate this higher stability against drainage for the mixture with the higher E_d and E_v values observed in Fig. 5. In fact, it has been reported that the elastic and viscous behavior at the air–water interface are key parameters in determining foams stability [54–57].

The decrease of foam volume over time (Fig. 8) was similar for foams of single CMP or KO, up to 200 s; after that time CMP foam volume decreased faster than KO foam and totally collapsed at 700 s. The mixed foam was initially much more stable against collapse than KO or CMP foams. After 400 s foam volume decrease accelerated and the foam totally collapsed at around 850 s.

Fig. 9 shows the images of KO, CMP–KO and CMP foams throughout aging time (500 s for KO and CMP–KO foams and 300 s for CMP foam). The images of the bubbles clearly reveal the high homogeneity and stability of air bubbles in KO foam as compared to CMP foam. The mixed foam looks more stable than CMP foam but it was more heterogeneous than KO foam indicating the influence of CMP on the structure of the bubbles but also the influence of KO that delays the increase of bubbles and foam collapse.

4. Conclusions

The addition of the surface–active polysaccharide (0.5 wt%) did not alter the foaming capacity of CMP (4 wt%) but strongly increased foam stability against drainage and collapse. Moreover, the liquid drainage and the initial foam collapse of mixed foam were much more retarded than what could be expected from the behavior of foams of single CMP or KO. This behavior could be related to the synergistic increase in the dilatational elasticity (E_d) and viscosity (E_v) of mixed films, which could be more resistant to drainage and rupture.

Thus the use of PGA in CMP foams could be a good strategy to improve its stability.

Acknowledgments

This research was supported by CYTED through project A.1.2. Universidad de Buenos Aires, Agencia Nacional de Promoción Científica y Tecnológica and Consejo Nacional de Investigaciones Científicas y Técnicas de la República Argentina. CICYT (Spain) through grant AGL2007-60045, and Consejería de Educación y Ciencia, Junta de Andalucía (Spain), through grant PO6-AGR-01535.

References

[1] C. Thomä-Worringer, J. Sørensen, R. López Fandiño, Health effects and technological features of caseinomacropeptide, Int. Dairy J. 16 (2006) 1324.
[2] M.H.A. El-Salam, S. El-Shibiny, W. Buchheim, Characteristics and potential uses of the casein macropeptide, Int. Dairy J. 6 (1996) 327.
[3] M. Miguel, M.A. Manso, R. López-Fandiño, M.J. Alonso, M. Salaices, Vascular effects and antihypertensive properties of [kappa]-casein macropeptide, Int. Dairy J. 17 (2007) 1473.
[4] M.J. Martinez, C. Carrera Sánchez, J.M. Rodríguez Patino, A.M.R. Pilosof, Bulk and interfacial behaviour of caseinoglycomacropeptide (GMP), Colloids Surf. B: Biointerfaces 71 (2009) 230.
[5] M.J. Martinez, C. Carrera Sánchez, J.M. Rodríguez Patino, A.M.R. Pilosof, Interactions in the aqueous phase and adsorption at the air–water interface of caseinoglycomacropeptide (GMP) and β-lactoglobulin mixed systems, Colloids Surf. B: Biointerfaces 68 (2009) 39.
[6] C. Thomä Worringer, J. Sørensen, R. López Fandiño, Health effects and technological features of caseinomacropeptide, Int. Dairy J. 16 (2006) 1324.
[7] C. Thomä Worringer, N. Siegert, U. Kulozik, Foaming properties of caseinomacropeptide. 2. Impact on pH and ionic strength, Milchwissenschaft 62 (2007) 253.
[8] M. Kreuβ, T. Strixner, U. Kulozik, The effect of glycosylation on the interfacial properties of bovine caseinomacropeptide, Food Hydrocolloids 23 (2009) (1818).
[9] M. Kreu, beta, I. Krause, U. Kulozik, Influence of glycosylation on foaming properties of bovine caseinomacropeptide, Int. Dairy J. 19 (2009) 715.
[10] R.I. Baeza, C. Carrera Sánchez, A.M.R. Pilosof, J.M. Rodríguez Patino, Interfacial and foaming properties of propylenglycol alginates. Effect of degree of esterification and molecular weight, Colloids Surf. B: Biointerfaces 36 (2004) 139.

[11] J.M. Rodríguez Patino, A.M.R. Pilosof, Protein–polysaccharide interactions at fluid interfaces, Food Hydrocolloids 25 (2011) (1925).
[12] E. Dickinson, An Introduction to Food Colloids, Oxford University Press, Oxford, UK, 1992.
[13] J.M. Rodríguez Patino, M.R. Rodríguez Niño, C. Carrera Sánchez, Protein–emulsifier interactions at the air–water interface, Curr. Opin. Colloid Interface Sci. 8 (2003) 387.
[14] J.L. Courthaudon, E. Dickinson, W.W. Christie, Competitive adsorption of lecithin and (-casein in oil-in-water emulsions, J. Agric. Food Chem. 39 (1991) 1365.
[15] A.R. Mackie, A.P. Gunning, P.S. Wilde, V.J. Morris, The orogenic displacement of proteins from the air–water interface by surfactant, J. Colloids Interface Sci. 210 (1999) 157.
[16] A.R. Mackie, A.P. Gunning, P.S. Wilde, V.J. Morris, Competitive displacement of β-lactoglobulin from the air–water interface by sodium dodecyl sulphate, Langmuir 16 (2000) 8176.
[17] R.I. Baeza, C. Carrera Sánchez, J.M. Rodríguez Patino, A.M.R. Pilosof, Interactions between β-lactoglobulin and polysaccharides at the air–water interface and the influence on foam properties, in: E. Dickinson (Ed.), Food Colloids. Interactions, Microstructure and Processing, The Royal Society of Chemistry, Cambridge, UK, 2005, p. 301.
[18] E. Dickinson, Hydrocolloids at interfaces and the influence on the properties of dispersed systems, Food Hydrocolloids 17 (2003) 25.
[19] K. Martínez, Impacto de la hidrólisis enzimática de las proteínas de soja en sus propiedades interfaciales, de espumado y en la interacción con polisacáridos, Departamento de Industrias, Facultad de Ciencias Exactas y Naturales, Universidad de Buenos Aires, PhD, Universidad de Buenos Aires, Buenos Aires, Argentina, 2007, p. 243.
[20] O.E. Pérez, C. Carrera Sánchez, J.M. Rodríguez Patino, A.M.R. Pilosof, Adsorption dynamics and surface activity at equilibrium of whey proteins and hydroxypropyl-methyl-cellulose mixtures at the air–water interface, Food Hydrocolloids 21 (2007) 794.
[21] R.I. Baeza, C. Carrera Sánchez, A.M.R. Pilosof, J.M. Rodríguez Patino, Interactions of polysaccharides with β-lactoglobulin adsorbed films at the air–water interface, Food Hydrocolloids 19 (2005) 239.
[22] R.I. Baeza, C. Carrera Sánchez, A.M.R. Pilosof, J.M. Rodríguez Patino, Interactions of polysaccharides with β-lactoglobulin spread monolayers at the air–water interface, Food Hydrocolloids 18 (2004) 959.
[23] M.R. Rodríguez Niño, C. Carrera Sánchez, M. Cejudo Fernández, J.M. Rodríguez Patino, Protein and lipid films at equilibrium at air–water interface, J. Am. Oil Chem. Soc. 78 (2001) 873.
[24] M.R. Rodríguez Niño, J.M. Rodríguez Patino, Effect of the aqueous phase composition on the adsorption of bovine serum albumin to the air–water interface, Ind. Eng. Chem. Res. 41 (2002) 1489.
[25] J.M. Rodríguez Patino, M.R. Rodríguez Niño, C. Carrera Sánchez, Adsorption of whey protein isolate at the air–water interface as a function of processing conditions: a rheokinetic study, J. Agric. Food Chem. 47 (1999) 2241.
[26] J. Lucassen, M. Van Den Tempel, Dynamic measurements of dilational properties of a liquid interface, Chem. Eng. Sci. 27 (1972) 1283.
[27] M.J. Martinez, C. Carrera Sánchez, J.M. Rodríguez Patino, A.M.R. Pilosof, Interactions between β-lactoglobulin and casein glycomacropeptide on foaming, Colloids Surf. B: Biointerfaces 89 (2012) 234.
[28] J.M. Rodríguez Patino, M.R. Rodríguez Niño, J.M. Álvarez Gómez, Interfacial and foaming characteristics of protein–lipid systems, Food Hydrocolloids 11 (1997) 49.
[29] M.R. Rodríguez Niño, J.M. Rodríguez Patino, Surface tension of protein and insoluble lipids at the air–aqueous phase interface, J. Am. Oil Chem. Soc. 75 (1998) 1233.
[30] J. Benjamins, Static and dynamic properties of protein adsorbed at liquid interfaces, Laboratorium voor Fysische chemie en kolloïdkunde, vol Ph.D., University of Wageningen Wageningen, The Netherlands, 2000.
[31] O.E. Pérez, C. Carrera Sanchez, J.M. Rodríguez Patino, A.M.R. Pilosof, Thermodynamic and dynamic characterization of hydroxypropylmethylcellulose adsorbed films at the air water interface, Biomacromolecules 7 (2006) 388.
[32] J.M. Álvarez Gómez, J.M. Rodríguez Patino, Formulation engineering of food model foams containing diglycerol esters and β-lactoglobulin, Ind. Eng. Chem. Res. 45 (2006) 7510.
[33] J.M. Rodríguez Patino, C. Carrera Sánchez, M.R. Rodríguez Niño, Physicochemical properties of surfactant and protein films, Curr. Opin. Colloid Interface Sci. 12 (2008) 187.
[34] D.E. Graham, M.C. Philips, Proteins at liquid interfaces: II. Adsorption isotherms, J. Colloid Interface Sci. 70 (1979) 415.
[35] D.E. Graham, M.C. Phillips, Proteins at liquid interfaces: III. Molecular structures of adsorbed films, J. Colloid Interface Sci. 70 (1979) 427.
[36] F. MacRitchie, A.E. Alexander, Kinetics of adsorption of proteins at interfaces. Part III. The role of electrical barriers in adsorption, J. Colloid Sci. 18 (1963) 464.
[37] S. Damodaran, K.B. Song, Kinetics of adsorption of proteins at interfaces: role of protein conformation in diffusional adsorption, Biochim. Biophys. Acta 954 (1988) 253.
[38] F. MacRitchie, Chemistry at Interfaces, Academic Press, San Diego, CA, 1990.
[39] F. MacRitchie, Proteins at interfaces, Adv. Protein Chem. 32 (1978) 283.
[40] E. Tornberg, The application of the drop volume technique to measurements of the adsorption of proteins at interface, J. Colloid Interface Sci. 64 (1978) 391.
[41] A.F.H. Ward, L. Tordai, Time-dependence of boundary tensions of solutions I. The role of diffusion in time-effects, J. Chem. Phys. 14 (1946) 453.
[42] O.E. Pérez, C. Carrera Sánchez, J.M. Rodríguez Patino, A.M.R. Pilosof, Dynamics of adsorption of hydroxypropyl methylcellulose at the air–water interface, Food Hydrocolloids 22 (2008) 387.
[43] S. Xu, S. Damodaran, Kinetics of adsorption of protein at the air–water interface from a binary mixture, Langmuir 10 (1994) 472.
[44] J.A. de Feijter, J. Benjamins, Adsorption kinetics of proteins at the air–water interface, in: E. Dickinson (Ed.), Food Emulsions and Foams, Royal Society of Chemistry, London, 1987, p. 72.
[45] W.W. Nawar, Food Chemistry, Marcel Dekker, New York, 1985 (Chapter 5).
[46] R.I. Baeza, A.M.R. Pilosof, C. Carrera Sánchez, J.M. Rodríguez Patino, Adsorption and rheological properties of biopolymers at the air–water interface, AIChE J. 52 (2006) 2627.
[47] D.K. Sarker, P.J. Wilde, Restoration of protein foam stability through electrostatic propylene glycol alginate-mediated protein–protein interactions, Colloids Surf. B: Biointerfaces 15 (1999) 203.
[48] R.A. Ganzevles, M.A. Cohen Stuart, T. van Vliet, H.H.J. de Jongh, Use of polysaccharides to control protein adsorption to the air–water interface, Food Hydrocolloids 20 (2006) 872.
[49] R.A. Ganzevles, K. Zinoviadou, T. van Vliet, M.A. Cohen Stuart, H.H.J. de Jongh, Modulating surface rheology by electrostatic protein/polysaccharide interactions, Langmuir 22 (2006) 10089.
[50] C. Schmitt, E. Kolodziejczyk, M.E. Leser, Interfacial and foam stabilization properties of β-lactoglobulin—acacia gum electrostatic complexes, in: E. Dickinson (Ed.), Food Colloids: Interactions, Microstructure and Processing, Royal Society of Chemistry, Cambridge, 2005, p. 289.
[51] L.S. Jourdain, C. Schmitt, M.E. Leser, B.S. Murray, E. Dickinson, Mixed layers of sodium caseinate + dextran sulfate: influence of order of addition to oil–water interface, Langmuir 25 (2009) 10026.
[52] J.N. Miquelim, C.S. Lannes, R. Mezzenga, pH influence on the stability of foams with protein–polysaccharide complexes at their interfaces, Food Hydrocolloids 24 (2010) 398.
[53] R.J. Pugh, Experimental techniques for studying the structure of foams and froths, Adv. Colloid Interface Sci. 114–115 (2005) 239.
[54] J. Maldonado-Valderrama, A. Martín-Rodriguez, M.J. Gálvez-Ruiz, R. Miller, D. Langevin, M.A. Cabrerizo-Vílchez, Foams and emulsions of β-casein examined by interfacial rheology, Colloids Surf. A: Physicochem. Eng. Aspects 323 (2008) 116.
[55] J. Maldonado-Valderrama, J.M. Rodríguez Patino, Interfacial rheology of protein–surfactant mixtures, Curr. Opin. Colloid Interface Sci. 15 (2010) 271.
[56] P.A. Wierenga, H. Gruppen, New views on foams from protein solutions, Curr. Opin. Colloid Interface Sci. 15 (2010) 365.
[57] J.M. Rodrïïguez Patino, C. Carrera Sánchez, M.R. Rodrïïguez Niño, Implications of interfacial characteristics of food foaming agents in foam formulations, Adv. Colloid Interface Sci. 140 (2008) 95.